Monatshefte für Chemie 138, 101–105 (2007)
DOI 10.1007/s00706-006-0572-3
Printed in The Netherlands

Monatshefte für Chemie
Chemical Monthly

Syntheses and Structure of $Er_6Co_{2.19(1)}In_{0.81(1)}$

Vasyl' I. Zaremba[1], **Yaroslav M. Kalychak**[1], **Mariya V. Dzevenko**[1], **Ute Ch. Rodewald**[2], **Rolf-Dieter Hoffmann**[2], and **Rainer Pöttgen**[2,*]

[1] Inorganic Chemistry Department, Ivan Franko National University, Lviv, Ukraine
[2] Institut für Anorganische und Analytische Chemie, Westfälische Wilhelms-Universität Münster, Münster, Germany

Received May 30, 2006; accepted (revised) July 4, 2006; published online January 2, 2007

Summary. The erbium–cobalt–indide $Er_6Co_{2.19(1)}In_{0.81(1)}$ was prepared by arc-melting of the pure elements. Single crystals were obtained through a special annealing procedure. $Er_6Co_{2.19(1)}In_{0.81(1)}$ crystallizes with the orthorhombic Ho_6Co_2Ga structure: *Immm*, $a = 934.3(1)$, $b = 936.4(1)$, $c = 985.4(1)$ pm, $wR2 = 0.0557$, 892 F^2 values, and 35 variable parameters. The structure contains two crystallographically independent Co_2 dumb-bells at Co–Co distances of 223 and 236 pm, respectively. Further structural motifs are distorted octahedral Er_6 clusters (336–401 pm Er–Er) which are condensed to a three-dimensional network *via* all corners. The In2 atoms have a distorted icosahedral erbium coordination (329–355 pm In2–Er). These icosahedra show an orthorhombically distorted *bcc* packing.

Keywords. Indium compounds; Intermetallics; Crystal chemistry.

Introduction

Three main motifs of chemical bonding can be distinguished for the large family of rare earth (*RE*) – transition metal (*T*) – indium compounds $RE_xT_yIn_z$ [1]. Most $RE_xT_yIn_z$ compounds with a sufficiently high transition metal and indium content build up two- or three-dimensional $[T_yIn_z]$ networks with significant covalent *T*–In bonding. The more electropositive rare earth metal atoms fill cages or channels left by these networks. A special case of these networks concerns the indium-rich materials, where the indium substructures already resemble the structure of elemental indium, *i.e.* distorted *bcc* indium fragments occur. Prominent examples are the indides $RETIn_4$ [2, 3], $EuRh_2In_8$ [4], or $RETIn_5$ [5–7, and refs. therein]. These materials have intensively been investigated with respect to their structural chemistry and physical properties and the literature has been reviewed recently [1].

When going to the transition metal-rich and rare earth metal-rich parts of the phase diagrams *RE*–*T*–In, only few structural information is available. The *T*-rich materials show strong clustering of the transition metal atoms, resulting in 1D-, 2D-, or 3D cluster units [8, 9, and refs. therein]. The rare earth metal-rich indium compounds display the typical structural chemistry of intermetallics compounds. Most atoms have high coordination numbers and the complex structures can be described by simple packing motifs of polyhedra [10, 11]. So far, the *RE*-rich phases $RE_{12}Ni_6In$ (*RE* = Y, La, Pr, Nd, Sm, Gd) and $RE_{12}Co_6In$ (*RE* = La, Pr, Nd, Sm) with $Sm_{12}Ni_6In$ type [10–12], RE_6Co_2In (*RE* = Sc, Y, Sm, Gd–Ho, Tm, Lu) with Ho_6Co_2Ga structure [11, 13–15], $RE_{14}Co_3In_3$ (*RE* = Y, Gd–Tm, Lu) [16–18] and $RE_{14}Ni_3In_3$ (*RE* = Sc, Y, Gd–Tm, Lu) [19] with $Lu_{14}Co_2In_3$ type, Er_5Ni_2In and $Tm_{4.83(3)}Ni_2In_{1.17(3)}$ [20] with Mo_5SiB_2 structure, and the series $RE_{12}Pt_7In$ (*RE* = Ce, Pr, Nd, Gd, Ho) [21] have been reported. During our recent investigation of the Er–Co–In system we obtained the new erbium-rich indide $Er_6Co_{2.19}In_{0.81}$ reported herein.

---

[*] Corresponding author. E-mail: pottgen@uni-muenster.de

Discussion

The crystal structure of $Er_6Co_{2.19}In_{0.81}$ (Tables 1–3) completes the series of RE_6Co_2In indides [11, 13–15]. These compounds adopt all the orthorhombic Ho_6Co_2Ga type structure [25], space group *Immm*. The course of the cell volumes of the RE_6Co_2In series is presented in Fig. 1. Three features need to be mentioned: (i) the volume of the scandium compound is the by far smallest in the whole series, (ii) the yttrium volume fits in between the volumes for the gadolinium and terbium compound, and (iii) the deviation from a smooth curve manifests the small homogeneity ranges $RE_6Co_{2+x}In_{1-x}$. Besides the indides, also the gallides RE_6Co_2Ga and RE_6Ni_2Ga [26], some stannides RE_6Ni_2Sn [26], and the plumbides $RE_6Co_{2+x}Pb_{1-y}$ (RE = Y, Gd–Tm, Lu) and $RE_6Ni_{2+x}Pb_{1-y}$ (RE = Tb–Tm, Lu) [27] have been reported. All indides show nearly the same composition for the crystals investigated, *i.e.* $Ho_6Co_{2.135}In_{0.865}$ [13], $Er_6Co_{2.19}In_{0.81}$ and $Sc_6Co_{2.18}In_{0.82}$ [15]. This is also supported by the preparative work of *Canepa et al.* [14]. They only obtained homogeneous samples of the gadolinium based compound for a composition $Gd_6Co_{2.2}In_{0.8}$. The plumbides differ from this behavior. Most of them additionally show defects on the 4*j* transition metal sites [27]. The reasons of the complex crystal chemistry of these materials certainly result from a complex interplay of geometric and electronic factors.

Table 1. Crystal data and structure refinement for $Er_6Co_{2.19(1)}In_{0.81(1)}$

Empirical formula	$Er_6Co_{2.19(1)}In_{0.81(1)}$
Structure type	Ho_6Co_6Ga
Z	4
Molar mass	1236.24 g/mol
Space group	*Immm*
Unit cell dimensions	$a = 934.3(1)$ pm
(single crystal data,	$b = 936.4(1)$ pm
high angle refinement)	$c = 985.4(1)$ pm
	$V = 0.8621\ nm^3$
Calculated density	$9.53\ g/cm^3$
Crystal size	$60 \times 60 \times 80\ \mu m^3$
Transm. ratio (max/min)	0.265/0.035
Absorption coefficient	$64.0\ mm^{-1}$
$F(000)$	2044
θ range	3° to 35°
Range in *hkl*	±14, ±15, ±15
Total no. of reflections	6494
Independent reflections	1068 ($R_{int} = 0.0455$)
Reflections with $I > 2\sigma(I)$	892 ($R_\sigma = 0.0350$)
Data/parameters	892/35
Goodness-of-fit on F^2	0.968
Final R indices $[I > 2\sigma(I)]$	$R1 = 0.0250$
	$wR2 = 0.0540$
R indices (all data)	$R1 = 0.0346$
	$wR2 = 0.0557$
Extinction coefficient	0.00143(6)
Largest diff. peak and hole	$3.34/-4.51\ e/Å^3$

Figure 2 gives two different views of the $Er_6Co_{2.19}In_{0.81}$ structure approximately along the *c* axis. The condensed distorted Er_6 octahedra are emphasized in the right-hand part of that figure. These empty octahedra are connected *via* all corners. The Er–Er distances cover the broad range from 336 to 401 pm. Some of these distances are even shorter than in *hcp* erbium [28] (6 × 347 and 6 × 356 pm), and we can safely assume a significant degree of Er–Er bonding, as expected for such a lanthanoid-rich compound. Similar range of *RE*–*RE* distances also occurs for the $RE_{14}Co_3In_3$ [16–18] compounds. The Er3 site has slightly enhanced displacement parameters ($U_{11} = 63(2)$, $U_{22} = 129(2)$, and $U_{33} = 177(2)\ pm^2$),

Table 2. Atomic coordinates and isotropic displacement parameters (pm^2) of $Er_6Co_{2.19(1)}In_{0.81(1)}$; U_{eq} is defined as one third of the trace of the orthogonalized U_{ij} tensor

Atom	*Wyckoff* site	Occ.	x	y	z	U_{eq}
$Er_6Co_{2.19(1)}In_{0.81(1)}$						
Er1	8*n*	1.00	0.28517(5)	0.18704(4)	0	85(1)
Er2	8*m*	1.00	0.30039(4)	0	0.31540(4)	68(1)
Er3	8*l*	1.00	0	0.20469(4)	0.22920(5)	123(1)
Co1	4*j*	1.00	1/2	0	0.1132(2)	84(3)
Co2	4*g*	1.00	1/2	0.1262(2)	1/2	105(3)
In1	2*a*	0.64(1)	0	0	0	117(5)
Co3	2*a*	0.36	0	0	0	117
In2	2*c*	1.00	0	0	1/2	68(2)

Table 3. Interatomic distances (pm) in $Er_6Co_{2.19(1)}In_{0.81(1)}$; standard deviations are all equal or less than 0.4 pm; all distances within the first coordination spheres are listed; *M* denotes 64% In1 + 36% Co3 (see Table 2)

Er1:	2	Co1	288.8	Er3:	1	Co2	275.9
	1	Co2	318.7		1	*M*	296.2
	1	*M*	318.8		1	Co1	317.2
	2	Er3	349.0		1	In2	328.6
	2	Er3	349.7		2	Er2	336.4
	1	Er1	350.3		2	Er1	349.0
	2	Er2	354.1		2	Er1	349.7
	1	In2	355.2		2	Er2	350.3
	2	Er2	357.0		1	Er3	383.3
	1	Er1	401.4	Co1:	1	Co	223.0
Er2:	1	Co	272.9		2	Er2	272.9
	2	Co	286.1		4	Er1	288.8
	1	In2	334.5		2	Er3	317.2
	2	Er3	336.4	Co2:	1	Co	236.3
	2	Er3	350.3		2	Er3	275.9
	2	Er1	354.1		4	Er2	286.1
	2	Er1	357.0		2	Er1	318.7
	1	Er2	363.8	*M*:	4	Er3	296.2
	1	Er2	373.0		4	Er1	318.8
					2	Co	350.1
				In2:	4	Er3	328.6
					4	Er2	334.5
					4	Er1	355.2

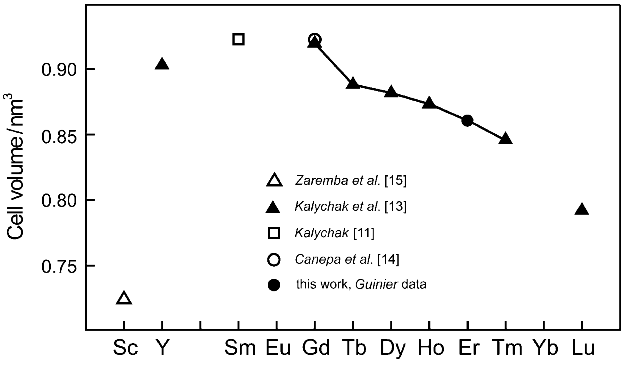

Fig. 1. Plot of the cell volumes of the orthorhombic indides $RE_6Co_{2+x}In_{1-x}$

however, this site is fully occupied. This behaviour is most likely a consequence of the shorter Er3–*M* distance (296 pm) as compared to Er1–*M* (319 pm), caused by the In1/Co3 mixing.

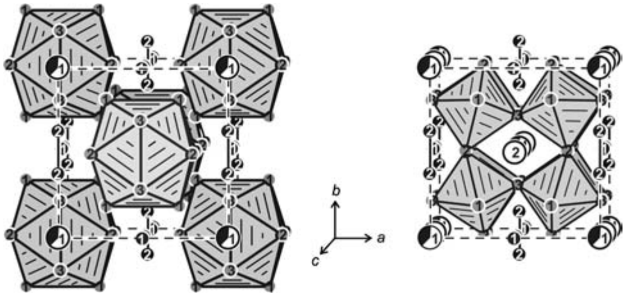

Fig. 2. View of the $Er_6Co_{2.19}In_{0.81}$ structure approximately along the *z* axis; erbium, cobalt, and indium atoms are drawn as grey, filled, and open circles, respectively; the mixed-occupied In1/Co3 site at the origin of the cell is shown with segments; the distorted erbium icosahedra around the In2 atoms are emphasized in the left hand drawing and the distorted octahedral erbium clusters and the two crystallographically independent Co_2 dumb-bells are emphasized in the right-hand part

Between the 3D network of Er_6 octahedra we observe two crystallographically independent Co_2 dumbells, the In2 and the mixed occupied In1/Co3 sites (Fig. 2). The $Co1_2$ dumb-bells (223 pm) extend in the *c* and the $Co2_2$ dumb-bells (236 pm) within the *b* direction. Both Co–Co distances are significantly smaller than the average Co–Co distance of 250 pm in *hcp* cobalt [28], and we can assume strong Co–Co bonding within these units.

The In2 atoms have distorted icosahedral erbium coordination (Fig. 2) in an orthorhombic body-centered packing. These icosahedra fill the space left by the network of erbium octahedra. For further crystal chemical details we refer to Ref. [15].

Experimental

Synthesis

Starting materials for the preparation of Er_6Co_2In were erbium ingots (Johnson-Matthey), cobalt powder (Sigma-Aldrich, 100 mesh), and indium tear drops (Johnson-Matthey), all with stated purities better than 99.9%. A sample of the nominal composition of Er_6Co_2In was synthesized from the pure elements by arc-melting [22]. In the first step the larger erbium ingots were cut into smaller pieces under paraffin oil. They were subsequently washed with *n*-hexane and kept under argon atmosphere prior to use. The paraffin oil and *n*-hexane have been dried over sodium wire. The argon was purified before over titanium sponge (900 K), silica gel, and molecular sieves. The amount of cobalt powder was cold-pressed to a small pellet (Ø = 6 mm).

The erbium pieces were then arc-melted to small buttons under an argon atmosphere. Subsequently the melted erbium button was mixed with the cold-pressed cobalt pellet and pieces of the indium tear drops in the ideal 6:2:1 atomic ratio and arc-melted. The sample was re-melted three times in order to ensure homogeneity. The total weight loss after the melting procedures was smaller than 0.5 wt%. After the arc-melting procedure the sample was obtained only in polycrystalline form.

Single crystals were grown *via* a special annealing mode. First the arc-melted sample was powdered and cold-pressed into a pellet. Next, the sample was put in a small tantalum container that has been sealed in an evacuated silica tube as an oxidation protection. The ampoule was first heated to 1300 K within 6 h and held at that temperature for another 6 h. Subsequently the temperature was lowered at a rate of 4 K/h to 1100 K, then at a rate of 10 K/h to 800 K, and finally cooled to room temperature within 10 h. After cooling, the samples could easily be separated from the tantalum container. No reaction of the sample with tantalum could be detected. As a result, single crystals of irregular shape were obtained and they exhibited metallic lustre.

Scanning Electron Microscopy

The single crystal investigated on the diffractometer has been analyzed by EDX measurements using a LEICA 420 I scanning electron microscope with ErF_3, elemental cobalt, and InAs as standards. No impurity elements were detected. Various point analyses on the crystal revealed the composition 65 ± 3 at% Er: 29 ± 3 at% Co: 6 ± 3 at% In, close to the values obtained from the structure refinement. The standard uncertainty accounts for the analyses at different points of the irregularly shaped crystal.

X-Ray Film Data and Structure Refinement

The sample was characterized through a *Guinier* powder patterns using Cu $K\alpha_1$ radiation and α-quartz ($a = 491.30$, $c = 540.46$ pm) as an internal standard. The *Guinier* camera was equipped with an imaging plate system (Fujifilm BAS-1800). The orthorhombic lattice parameters ($a = 934.2(2)$, $b = 935.7(3)$, $c = 984.2(3)$ pm) were deduced from least-squares fits of the powder data. The correct indexing of the powder pattern was ensured through an intensity calculation [23] using the atomic positions obtained from the structure refinement. Since the a and b lattice parameters were almost identical, additionally the lattice parameters of the single crystal were refined from 25 carefully centered high-angle reflections leading to the data listed in Table 1.

Small, irregularly shaped single crystals of Er_6Co_2In were selected from the annealed sample and first examined by *Laue* photographs on a *Buerger* precession camera (equipped with an imaging plate system Fujifilm BAS-1800) in order to establish suitability for intensity data collection. Intensity data were collected at room temperature by use of a *Stoe* IPDS-II diffractometer with graphite monochromatized Mo $K\alpha$ radiation. The absorption corrections were numerical. All relevant crystallographic details for the data collection and evaluation are listed in Table 1.

The isotypy of Er_6Co_2In with the neighbouring RE_6Co_2In compounds [11, 13–15] was already evident from the *Guinier* data. The atomic positions of $Sc_6Co_{2.18}In_{0.82}$ [15] were taken as starting values and the structure was refined using SHELXL-97 (full-matrix least-squares on F_o^2) [24] with anisotropic atomic displacement parameters for all sites. Similar to the scandium compound, the 2a site also shows some Co/In mixing. This occupancy parameter was refined as a least-squares variable in the final cycles, leading to the composition $Er_6Co_{2.19(1)}In_{0.81(1)}$ for the investigated crystal. All other sites were fully occupied within two standard uncertainties. The refinement went smoothly to the residuals listed in Table 1. A final difference *Fourier* synthesis revealed no significant residual peaks (Table 1). The positional parameters and interatomic distances are listed in Tables 2 and 3. Further details on the structure refinement may be obtained from Fachinformationszentrum Karlsruhe, D-76344 Eggenstein-Leopoldshafen (Germany), by quoting the Registry No. CSD-416647.

Acknowledgements

We thank *H.-J. Göcke* for the work at the scanning electron microscope. This work was financially supported by the Deutsche Forschungsgemeinschaft.

References

[1] Kalychak YaM, Zaremba VI, Pöttgen R, Lukachuk M, Hoffmann R-D (2005) Rare Earth-Transition Metal-Indides. In: Gschneidner KA Jr, Pecharsky VK, Bünzli J-C (eds) Handbook on the Physics and Chemistry of Rare Earths, Elsevier, Amsterdam, Vol. 34, Chapter 218, 1–133

[2] Hoffmann R-D, Pöttgen R (2000) Chem Eur J **6**: 600

[3] Hoffmann R-D, Pöttgen R, Zaremba VI, Kalychak YaM (2000) Z Naturforsch **55b**: 834

[4] Pöttgen R, Kußmann D (2001) Z Anorg Allg Chem **627**: 55

[5] Moshopoulou EG, Fisk Z, Sarrao JL, Thompson JD (2001) J Solid State Chem **158**: 25

[6] Zaremba VI, Rodewald UCh, Pöttgen R (2003) Z Naturforsch **58b**: 805

[7] Williams WM, Pham L, MaQuilon S, Moldovan M, Fisk Z, Young DP, Chan JY (2006) Inorg Chem **45**: 4637

[8] Kalychak YaM, Zaremba VI, Galadzhun YaV, Miliyanchuk KhYu, Hoffmann R-D, Pöttgen R (2001) Chem Eur J **7**: 5343

[9] Zaremba VI, Kaczorowski D, Hoffmann R-D, Heying B, Pöttgen R (2006) Solid State Sci **8**: 716

[10] Kalychak YaM (1997) J Alloys Compd **262–263**: 341

[11] Kalychak YaM (1999) J Alloys Compd **291**: 80

[12] Kalychak YaM, Zaremba VI, Stępień-Damm J, Galadzhun YaV, Akselrud LG (1998) Kristallografia (in Russian) **43**: 17

[13] Kalychak YaM, Zaremba VI, Zavalii PYu (1993) Z Kristallogr **208**: 380

[14] Canepa F, Napoletano M, Manfrinetti P, Merlo F (2002) J Alloys Compd **334**: 34

[15] Zaremba RI, Kalychak YaM, Rodewald UCh, Pöttgen R, Zaremba VI (2006) Z Naturforsch **61b**: 942

[16] Zaremba VI, Kalychak YaM, Zavalii PYu (1992) Sov Phys Crystallogr **37**: 178

[17] Canepa F, Napoletano M, Fornasini ML, Merlo F (2002) J Alloys Compd **345**: 42

[18] Zaremba VI, Kalychak YaM, Dzevenko MV, Rodewald UCh, Heying B, Pöttgen R (2006) Z Naturforsch **61b**: 23

[19] Lukachuk M, Galadzhun YaV, Zaremba RI, Dzevenko MV, Kalychak YaM, Zaremba VI, Rodewald UCh, Pöttgen R (2005) J Solid State Chem **178**: 2724

[20] Lukachuk M, Kalychak YaM, Dzevenko M, Pöttgen R (2005) J Solid State Chem **178**: 1247
[21] Galadzhun YaV, Zaremba VI, Kalychak YaM, Davydov VM, Pikul AP, Stępień-Damm J, Kaczorowski D (2004) J Solid State Chem **177**: 17
[22] Pöttgen R, Gulden Th, Simon A (1999) GIT Labor Fachzeitschrift **43**: 133
[23] Yvon K, Jeitschko W, Parthé E (1977) J Appl Crystallogr **10**: 73
[24] Sheldrick GM (1997) SHELXL-97, Program for Crystal Structure Refinement, University of Göttingen
[25] Gladyshevskii RE, Grin YuN, Yarmolyuk YaP (1983) Dopov Akad Nauk Ukr RSR Ser A **45**: 67
[26] Sichevich OM, Komarovskaja LP, Grin YuN, Yarmolyuk YaP, Skolozdra RV (1984) Ukr Fiz Zh **29**: 1342
[27] Gulay LD, Wołcyrz M (2001) J Alloys Compd **315**: 164
[28] Donohue J (1974) The Structures of the elements. Wiley, New York